Erratum: On seismic ambient noise cross-correlation and surface-wave attenuation

Lapo Boschi, Fabrizio Magrini, Fabio Cammarano, Mark van Der Meijde

Geophysical Journal International

Geophys. J. Int. (2020) **222,** 1090–1092 doi: 10.1093/gji/ggaa225
Erratum

Erratum: On seismic ambient noise cross-correlation and surface-wave attenuation

by Lapo Boschi,[1,2,3] Fabrizio Magrini,[4] Fabio Cammarano[4] and Mark van der Meijde[5]

[1] *Dipartimento di Geoscienze, Università degli Studi di Padova, Italy. E-mail: lapo.boschi@unipd.it*
[2] *Sorbonne Université, CNRS, INSU, Institut des Sciences de la Terre de Paris, ISTeP UMR 7193, F-75005 Paris, France*
[3] *Istituto Nazionale di Geofisica e Vulcanologia, Sezione di Bologna, Via Donato Creti 12, 40128 Bologna, Italy*
[4] *Department of Geological Science, Università degli Studi Roma Tre, Italy*
[5] *Faculty of Geo-Information Science and Earth Observation (ITC), University of Twente, The Netherlands*

in original form 2020 March 19

Key words: Theoretical seismology; Seismic attenuation; Seismic noise; Surface waves and free oscillations; Seismic interferometry.

Upon numerical testing of our earlier theoretical results, we found a trivial algebraic error in Boschi *et al.* (2019), that had an impact on the numerical results published in that article. In the following, we describe the error and summarize the corrections that should be applied to the results.

Eq. (A20) in Boschi *et al.* (2019) is obtained by inverse Fourier transforming $i\omega$ (with i denoting the imaginary unit, and ω frequency) to the time domain; it is implied that the inverse Fourier transform of $i\omega$ is $\delta'(t)$, where δ' is the derivative of the Dirac delta function, and t is time. However, based on the definition of Fourier transform given by Boschi & Weemstra (2015) and employed throughout Boschi *et al.* (2019), the inverse Fourier transform of $i\omega$ is $\sqrt{2\pi}\delta'(t)$. (This can be proved, for example, by replacing $f(t)$ with $\delta'(t)$ in the definition of Fourier transform, eq. (B1) of Boschi & Weemstra (2015), and applying the properties of $\delta'(t)$.) In other words, Boschi *et al.* (2019) have neglected a factor $\sqrt{2\pi}$ that should appear at the right-hand sides of eqs (A20), (A21) and (A22).

In section 2.2, eq. (A22) was used in the derivation of eq. (16), which, as a result, also lacks a factor $\sqrt{2\pi}$ at the left-hand side, i.e. it should be replaced by

$$\frac{2\sqrt{2\pi}\alpha\omega c}{P}\int_{\mathbb{R}^2} d^2\mathbf{x}\, G_{2D}^d(\mathbf{x},\mathbf{x}_A,\omega)G_{2D}^{d*}(\mathbf{x},\mathbf{x}_B,\omega) = -\Im[G_{2D}^d(\mathbf{x}_A,\mathbf{x}_B,\omega)], \quad (1)$$

where G_{2D}^d is the "damped" Green's function of Boschi *et al.* (2019), α the attenuation parameter as defined by Boschi *et al.* (2019), P a constant factor accounting for the physical dimensions of G_{2D}^d, c denotes phase velocity, and $\mathbf{x}$, $\mathbf{x}_A$, $\mathbf{x}_B$ are positions in space.

The error propagated to eq. (22) and, through the subsequent derivation, to eq. (30); the latter should be replaced by

$$\frac{s(\mathbf{x}_A,\omega)s^*(\mathbf{x}_B,\omega)}{<|s(\mathbf{x},\omega)|^2>_{\mathbf{x}}} \approx \frac{c}{\pi\omega I(\alpha,\omega,c)}J_0\left(\frac{\omega|\mathbf{x}_A-\mathbf{x}_B|}{c}\right)\frac{e^{-\alpha|\mathbf{x}_A-\mathbf{x}_B|}}{\alpha}, \quad (2)$$

where $s(\mathbf{x},\omega)$ is the Fourier transform of the signal recorded at a location $\mathbf{x}$; the average of its power-spectral density, $<|s(\mathbf{x},\omega)|^2>_{\mathbf{x}}$, is computed over all available receivers. J_0 denotes the zeroth-order Bessel function of the first kind (e.g. Boschi & Weemstra 2015). The cost functions C_1, C_2 and C_3 derived on the basis of eq. (30) also need to be corrected accordingly. (It is worth mentioning, on the other hand, that the derivation of eq. (28) in Boschi *et al.* (2019) does not rest on eq. (A22), and is therefore, to the best of our knowledge, error-free.)

As a result, the multiplicative factor relating normalized cross correlation to damped Bessel function, shown in Fig. 17 of Boschi *et al.* (2019), must be divided by $\sqrt{2\pi}$; it is then found to have values ranging between about 1.2–1, and very close to 1 at most frequencies.

Models $\alpha(\omega)$ derived by Boschi *et al.* (2019) also need to be corrected. Because we consider the cost function C_3 to be more effective than C_1 and C_2 at constraining α, we recomputed C_3 from the data of Boschi *et al.* (2019), after correcting its formula as follows,

$$C_3(\alpha,\omega) = \sum_{i,j} w(|\mathbf{x}_i-\mathbf{x}_j|)\left|\mathrm{env}\left[\frac{s(\mathbf{x}_i,\omega)s^*(\mathbf{x}_j,\omega)}{<|s(\mathbf{x},\omega)|^2>_{\mathbf{x}}}\right] - \mathrm{env}\left[\frac{c_{ij}(\omega)}{\pi\omega I[\alpha(\omega),\omega,c_{ij}(\omega)]}J_0\left(\frac{\omega|\mathbf{x}_i-\mathbf{x}_j|}{c_{ij}(\omega)}\right)\frac{e^{-\alpha|\mathbf{x}_i-\mathbf{x}_j|}}{\alpha}\right]\right|^2, \quad (3)$$

where the indexes i, j refer to different stations in the array, env[. . .] denotes the envelope function, the interstation-distance-dependent weight $w(|\mathbf{x}_i-\mathbf{x}_j|) = |\mathbf{x}_i-\mathbf{x}_j|^e$ and e is the Euler number.The results of this exercise are shown in Figs 1 and 2; we find the most probable values of

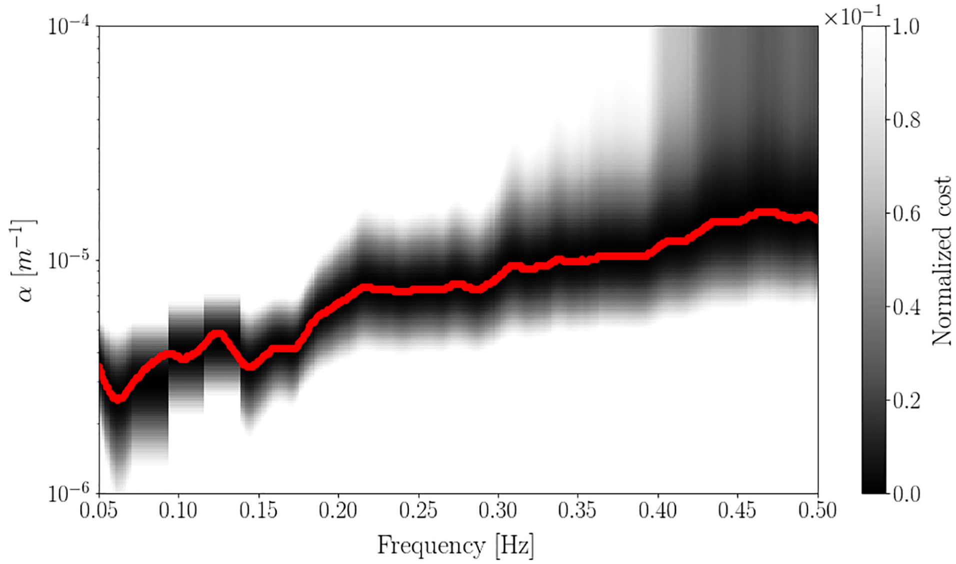

Figure 1. Cost function $C_3(\alpha, \omega)$ shown (after normalization) as a function of attenuation parameter and frequency. We normalize C_3 according to the formula $\frac{C_3(\alpha,\omega)-\min[C_3(\alpha,\omega)]}{\max[C_3(\alpha,\omega)]-\min[C_3(\alpha,\omega)]}$, where min $[C_3]$ and max $[C_3]$ denote the minimum and maximum values of C_3 for all sampled values of α and ω. A red curve marks the values of α for which C_3 is minimized at each frequency. The stepwise trend of the minima of C_3 is correlated with the stepwise growth (also as a function of ω) of the number of station pairs for which cross-correlation data are available. This figure replaces Fig. 14 of Boschi *et al.* (2019).

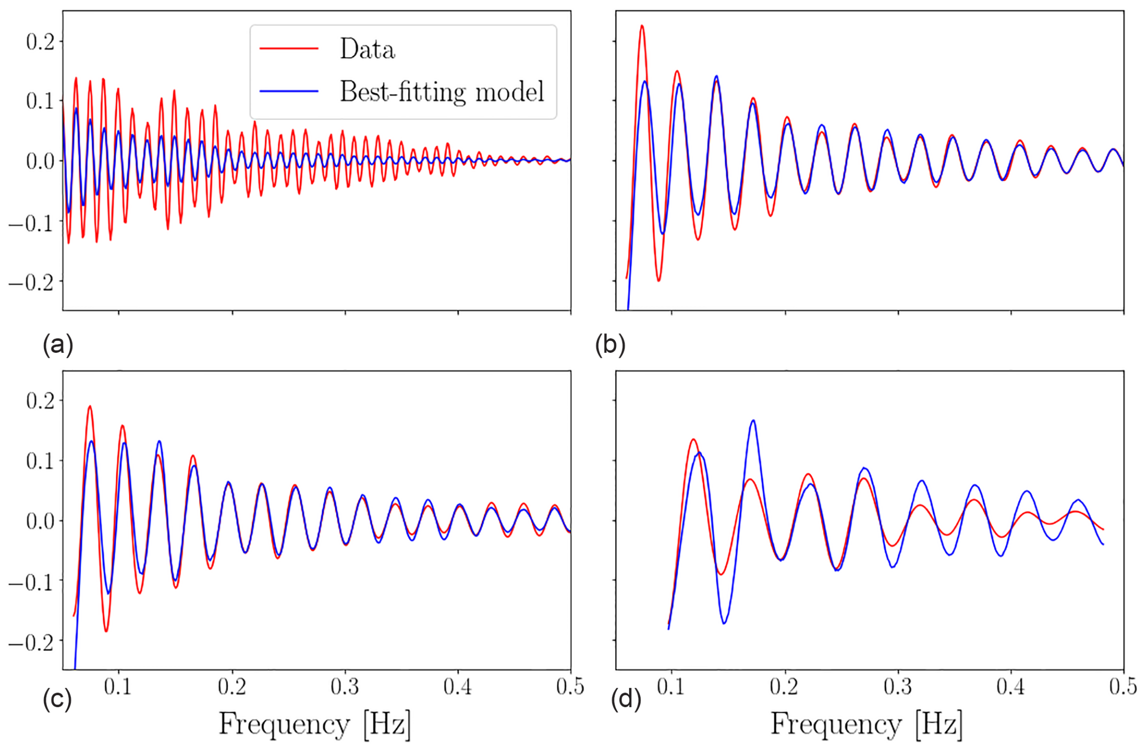

Figure 2. Comparison of normalized data (red lines) and model (blue), i.e. left- and right-hand side of eq. (2), after substituting the values of $\alpha(\omega)$ that minimize C_3 (Fig. 1). Panels a, b, c and d correspond to station pairs UT.006-UT.009, UT.002 - UT.004, IV.AGLI-IV.DGI and UT.002-UT.003 (Boschi *et al.* 2019), respectively, with interstation distances decreasing from 231 to 57 km. This figure replaces Fig. 16 of Boschi *et al.* (2019).

α to be on the order of 10^{-6}-10^{-5}, and rarely larger than 10^{-5}, in the period range 2-10 s. this is almost an order of magnitude smaller than the values found by Boschi *et al.* (2019), but close to the majority of independent estimates made in different areas of the globe (e.g. Mitchell 1995; Harmon *et al.* 2010; Lawrence & Prieto 2011; Lin *et al.* 2011; Romanowicz & Mitchell 2015).

In a new study by our team that is currently in preparation, eq. (28) of Boschi *et al.* (2019) and eq. (2) from this study are both validated numerically; synthetic tests show that, after correcting the errors, attenuation models $\alpha(\omega)$ can be retrieved successfully through the inversion procedure described by Boschi *et al.* (2019).

REFERENCES

Boschi, L. & Weemstra, C., 2015. Stationary-phase integrals in the cross-correlation of ambient noise, *Rev. Geophys.,* **53,** doi:10.1002/2014RG000455, 411-451.

Boschi, L., Magrini, F., Cammarano, F. & van der Meijde, M., 2019. On seismic ambient noise cross-correlation and surface-wave attenuation, *Geophys. J. Int.,* **219,** 1568–1589.

Harmon, N., Rychert, C. & Gerstoft, P., 2010. Distribution of noise sources for seismic interferometry, *Geophys. J. Int.,* **183,** 1470–1484.

Lawrence, J.F. & Prieto, G.A., 2011. Attenuation tomography of the western United States from ambient seismic noise, *J. Geophys. Res.,* **116,** B06302.

Lin, F.-C., Ritzwoller, M.H. & Shen, W., 2011. On the reliability of attenuation measurements from ambient noise cross-correlations, *Geophys. Res. Lett.,* **38,** L11303.

Mitchell, B.J., 1995. Anelastic structure and evolution of the continental crust and upper mantle from seismic surface wave attenuation, *Rev. Geophys.,* **33,** 441–462.

Romanowicz, B.A. & Mitchell, B.J., 2015. Deep earth structure: Q of the earth from crust to core, in *Treatise of Geophysics, Second Edition,* pp. 789–827, Elsevier, Amsterdam.